MRSE Materials Reports Solidwaste & Ecomaterials

Materials Reports: Solidwaste and Ecomaterials

Journal Homepage: www.sciopen.com/journal/3078-4093

Original Research Report

Producing belitic calcium sulfoaluminate cement without bauxite: using aluminium slag and waste clays

Vaishnav Kumar Shenbagam [1, *], Rand Hadi Farhan [1, 2], Theodore Hanein [1, *]

[1] School of Civil Engineering, University of Leeds, Leeds, LS2 9LG, UK

[2] Altek Europe, Chesterfield, S40 2UB, UK

Abstract: Locally available waste materials from the UK are used to synthesize belitic calcium sulfoaluminate (BCSA) clinker/cement. The raw materials (limestone, waste clay, and gypsum) were sourced locally, and additionally the non-metallic by-product (NMP) from the processed black dross (formed during the secondary aluminium production; aluminium scrap recycling) was used to boost alumina content. BCSA clinker with a target composition of approximately 60% belite and 30% ye'elimite was synthesised on a laboratory scale under varying clinkering conditions. The results show the possibility of using NMP and local materials available within the UK to produce BCSA cement without the need for bauxite. The clinker formation was found to be influenced by the raw materials used, in particular iron content and/or clay mineral type, and the clinkering conditions. The raw meal containing a higher amount of iron required a higher burning temperature or longer dwell time for the desired clinker chemistry to be obtained. The synthesized BCSA cement was hydrated with gypsum at a water-to-cement ratio of 0.5 to assess the reactivity of the binder. At 56 d, there was complete consumption of ye'elimite, and initial reaction of belite was observed with ettringite, aluminium hydroxide, and strätlingite forming as the main hydration products, demonstrating reactivity of both major clinker phases.

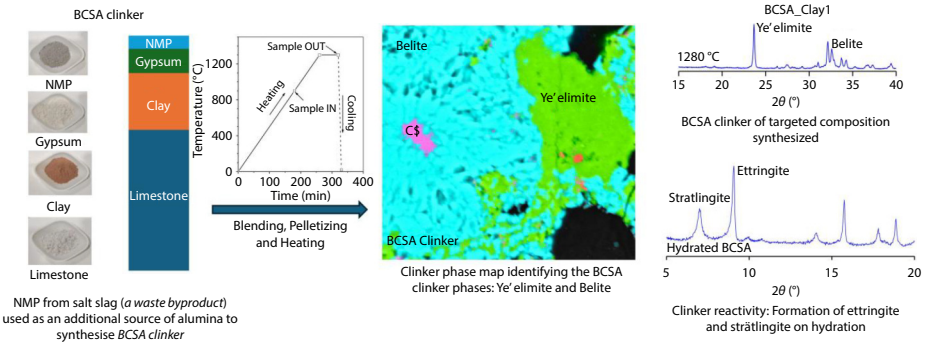

NMP from salt slag (*a waste byproduct*) used as an additional source of alumina to synthesise *BCSA clinker*

Clinker phase map identifying the BCSA clinker phases: Ye'elimite and Belite

BCSA clinker of targeted composition synthesized

Clinker reactivity: Formation of ettringite and strätlingite on hydration

Keywords: aluminium salt slag, aluminium recycling, non-metallic by-product, kaolinite, belitic calcium sulfoaluminate, clinker

Citation: V. K. Shenbagam, R. H. Farhan, T. Hanein. Producing belitic calcium sulfoaluminate cement without bauxite: using aluminium slag and waste clays. *Materials Reports: Solidwaste and Ecomaterials*, 2025, 1: 9520009. https://doi.org/10.26599/MRSE.2025.9520009.

1. Introduction

Cement is one of the most consumed materials with a global market size of ~400 billion USD, and approximately 4 billion metric tonnes of Portland-based cement are currently produced annually[1]. The cement manufacturing process is also considered responsible for approximately 8% of the global anthropogenic greenhouse gas emissions[2,3]. With the increasingly severe effects of global warming becoming catastrophic, global collaboration is essential to reduce CO_2 emissions from the cement industry through multiple fronts. The use of alternative low-CO_2 binders, such as calcium sulfoaluminate (CSA)-based binders[4], is a promising route to reducing the emissions associated with cement manufacture[5]. CSA-

*Correspondence to V. K. Shenbagam, v.kumarshenbagam@leeds.ac.uk; T. Hanein, T.Hanein@leeds.ac.uk

Received 5 November 2024; Received in revised form 13 February 2025; Accepted 1 March 2025

based cement requires lower energy and a lower quantity of calcium carbonate for manufacture compared to Portland cement (PC)[6]. These types of cement could also be more easily recyclable than PC systems blended with supplementary cementitious materials.

CSA-based binders usually have ye'elimite ($C_4A_3\$$), belite (C_2S), ferrite (C_4AF), and (an)hydrous calcium sulfate ($C\$$) as the primary clinker phases (cement chemistry notations: C=CaO, A=Al_2O_3, \$=SO_3, S=SiO_2, F=Fe_2O_3). CSA-based cement does not have a fixed composition and, based on the phase assemblage and quantities, can have different properties and be classified as different types of cement[7,8]. CSA was first introduced in the 1960s as an expansive additive to PC[9,10] and later transformed into several different binder systems. One example is the standalone binder known as belitic calcium sulfoaluminate (BCSA) cement with ye'elimite and belite as the primary clinker phases, while iron-rich variants have been named Belite-Ye'elimite-Ferrite (BYF) cement or ferroaluminate cement[4,11]. CSA cement is also known by several other names, including low-carbon cement, Klein's compound, and the third cement series. The main advantage today, apart from the lower-carbon nature, of CSA-based cement is its rapid hardening properties; these advantages are obvious when time is of the essence and the mortar/concrete needs to achieve the desired strength in a short time[12]. CSA cement has been widely used as a construction material in both structural and non-structural applications for decades in the USA and China, and further use of CSA cement as building materials is likely to spread in other countries depending on the availability of the raw materials[8,11]. Some examples of the use of CSA cement include concrete road repair, production of concrete pipes, using as a binder in concrete for bridges, airport runways, highways, long-span industrial floor slabs, and bridge decks[11,13,14].

BCSA has belite and ye'elimite as the primary clinker phases. The advantage of BCSA over cement richer in ye'elimite is that it can be produced from high-alumina (e.g., kaolinitic) clays, diminishing the need for scarce bauxite; this was first shown, including at scale, by Hanein et al.[15]. Ye'elimite is a highly hydraulic/reactive clinker phase, which contributes to the early-age hardening and strength gain properties[16,17]. As the lime-intense phases (C_3S) found in PC are replaced by ye'elimite to contribute to the early-age strength, there is a direct reduction in the carbon footprint stemming from limestone usage. The overall CO_2 emission reduction during the manufacturing of BCSA can be 25%–35% compared to that of PC manufacturing[6]. This can be attributed to the reduced limestone requirement and lower theoretical energy requirement (~200 °C lower kiln temperature) for the clinker formation. Furthermore, BCSA clinker has been reported to be more friable (porous) than PC clinker, reducing the grinding energy requirement[18].

The use of alternative raw materials such as industrial by-products can further help reduce the carbon footprint and promote landfill avoidance, thus improving circularity within the industrial sector[19]. BCSA has been shown to be made from alternative materials in several studies[20–29]. The use of alternative materials to synthesise clinkers also brings unconventional impurities or minor phases, which could affect the clinkering process and the reactivity of the clinker. BCSA, upon hydration (and sulfate availability), can form ettringite as the main hydration product[16], which has been used for immobilization and stabilization of several heavy metals through ionic substitution[30,31]. Gougar et al. term ettringite as a "very forgiving" phase, allowing for changes in its composition without altering the structure, thereby accommodating several (hazardous) ionic substitutions and chemical elements[32]. This facilitates the use of industrial by-products for synthesising the ye'elimite or BCSA cement. In addition to having a reduced carbon footprint, BCSA cement has also been used as special cement owing to its rapid hardening and self-stressing (expansive) properties[33,34]. The hydration of ye'elimite forms ettringite or calcium monosulfoaluminate based on the availability of calcium sulfate[17,35]. The rapid formation of ettringite at early ages contributes to the formation of a dense microstructure, providing early age hardening and strength development. The C_2S phase has been reported to form C-S-H (calcium silicate hydrate gel) or strätlingite at later ages, which can fill the pores and improve the long-term durability of the binder system[35,36].

The basic raw materials and major oxides needed for making BCSA cement are similar to those of PC, but BCSA requires a lower amount of limestone (CaO) and a higher amount of alumina and sulfate[37]. Limestone, clay, and gypsum, which are the primary sources of CaO, SiO_2, Al_2O_3, Fe_2O_3, and SO_3, are generally abundant; however, since BCSA requires a higher amount of Al_2O_3, additional alumina sources (conventionally bauxite) may be required depending on alumina content in the clay. One of the bottlenecks in the economic and large-scale production of BCSA could be the availability of economically viable sources of alumina[38]. The economic feasibility of CSA-based clinker was shown to depend highly on the source of bauxite, with CSA being cost-efficient when bauxite is sourced locally or imported from a short distance[39]. When bauxite, which is the common source of alumina, is not readily available, alternative alumina-rich sources have to be considered. In the literature, alternative sources such as red mud, alumina sludge, and slag have been used for synthesising BCSA clinker. The current study explores the possibility of using locally available by-products from the secondary aluminium production process.

The process of extracting aluminium from scrap metals is termed the secondary aluminium production process. As part of this process, typically, a salt flux is added with the scrap metal to the rotary furnace to reduce the metal oxides and remove impurities. The salt flux, along with the impurities (minor elements), is termed salt slag, which contains the salts, residual aluminium metal, aluminium oxides, nitrides, and chlorides. The salt slag is further refined in the tertiary aluminium process by leaching to extract all viable metal aluminium and removing the salt solution, which is used back in the secondary aluminium production process. The residue left is termed the non-metallic (by) product (NMP)[40]. NMP is still rich in aluminium, mostly in the oxide form, which is not

economically feasible to extract further. NMP is typically considered a waste product with not much economic value and is dumped in landfills at a cost[41]. Thus, using this material would provide additional benefits by reusing the by-products from the manufacturing line. The estimated secondary aluminium production in the UK is about 150000 metric tonnes[42]; for example, approximately seventy cans yield 1 kg of aluminium metal. The aluminium oxide residue from the secondary and tertiary aluminium production process (aluminium recycling) is readily available and will remain so for the foreseeable future[43]. The amount of salt slag generated from the secondary aluminium production is about 20%–50% of the weight of secondary aluminium, depending on the raw mix used for the process[40]. Depending on the composition of the salt slag (or black dross), each tonne of recycled black dross yields 200–500 kg of NMP[44,41]. The estimate of NMP available in the UK would then be between 15000 and 38000 metric tonnes annually, creating a perfect opportunity to use NMP in clinker production. Until now, NMP has only been used at low dosages in the production of PC [43,45]. For the first time, in this study, we use NMP with other locally available raw materials in the UK to manufacture BCSA.

The use of alternative materials in synthesising clinkers comes with its own set of challenges, mainly due to the unconventional elements or impurities present in them, which could affect the clinkering process and the reactivity of the clinker. This study focuses on understanding the effects of using limited amounts of NMP, along with two alternative local sources of clay from the UK, on the manufacturing and hydraulic reactivity of BCSA clinker. The raw materials were characterised, and their feasibility for use as a raw meal for BCSA clinker manufacturing was assessed. The microstructure of the produced clinker was then characterised with a focus on phase assemblage and tracing the presence of any potentially deleterious chemical elements. Microstructural characterization of the hydrated paste samples was also conducted to understand the fate of the minor elements and their effect on the reactivity of the BCSA binder system.

2. Materials and methods

2.1. Materials

The raw meal for the clinker was made using local limestone, waste clay from two different sources (termed Clay_1 and Clay_2), gypsum, and processed NMP as the main sources of CaO, Al_2O_3, SiO_2, SO_3 and the additional/top-up source of Al_2O_3, respectively, in the raw meal. The NMP is processed from salt slag; Clay_1 is from dewatering a waste stream from kaolin processing plants (always discarded as waste in modern operations), and Clay_2 is waste clay from railway construction.

The raw materials were calcined at 1000 °C for 3 h and then ground to a particle size of less than 63 μm after cooling to room temperature. Additionally, pure chemicals ($CaCO_3$, Al_2O_3, SiO_2, and $CaSO_4$) were used to synthesise BCSA to compare with the clinker made from the locally available and waste materials.

2.2. Analysis techniques

The elemental composition of the raw materials was determined by X-ray fluorescence spectroscopy (PANalytical Zetium). The samples were prepared as fused beads with a lithium-metaborate flux, and the quantification was done against the WROXY standard.

The clinker phase quantification was analyzed using quantitative X-ray diffraction (XRD). The diffractograms were collected by the PANalytical X'Pert and PANalytical Aeris instruments using a Cu-Kα X-ray source, in the 2θ range of 5° to 60° with a step size of 0.01° at the rate of about 30 s per step. All the samples were back-loaded to avoid preferred orientation, and the diffraction data were collected with continued rotation of the sample holder at 30 r min^{-1}. The clinker phase identification and quantification were performed using Rietveld refinement in TOPAS software. The refinement was done for different phases using the crystallographic information shown in Table 1. Refinement was conducted until Rwp (weighted pattern residual error) and GOF (goodness of fit) values reached below 10.0 and 5.0, respectively, to ensure a reliable quantification.

Simultaneous thermal analysis (STA) was carried out using a TA Instrument Q600 SDT, over the temperature range of 50 °C to 1300 °C (heating rate: 10 °C min^{-1}) in a constant air environment (flow rate: 100 mL min^{-1}). The samples were tested using an alumina crucible with an empty alumina crucible as a reference for baseline correction. The change in mass (TG) and heat flow (DSC) was monitored with the increasing temperature.

Spectroscopic mapping of clinker phases and distribution of the different elements was performed using scanning electron microscopy combined with energy dispersive spectroscopy (SEM-EDS). The pellets of clinker samples were broken into smaller chunks and used for testing in SEM. The samples were embedded in low-viscosity epoxy, and a polished section with ~10 nm carbon coating was used for the SEM

Table 1. Crystallographic information of the phases used in the Rietveld refinement.

Clinker phase	Crystal structure	ICDD No.
Ye'elimite ($C_4A_3\$$)	Orthorhombic	01-083-9042[46]
Belite (C_2S)	Monoclinic	04-007-2687[47]
Anhydrite (C$)	Orthorhombic	01-072-0916[48]
Ferrite (C_4AF)	Orthorhombic	01-074-3672[49]
Tricalcium aluminate (C_3A)	Cubic	00-038-1429[50]
Gehlenite (C_2AS)	Tetragonal	00-035-0755[51]
Ternesite ($C_5S_2\$$)	Orthorhombic	01-088-0812[52]

analysis. The SEM instrument Inspect F50 was used at 10 kV and 20 kV to obtain the backscattered electrons (BSE) imaging and EDS spectra.

2.3. Raw-mix preparation and pyroprocessing

The clinker phase composition was selected to reflect a BCSA binder system with a high belite content and lower amounts of ye'elimite (~30 wt%), which would be enough to provide high early-age strength and rapid hardening properties[13,15]. The raw meal design was based on stoichiometric calculations using the oxide composition of the raw materials obtained from XRF. The raw materials were batched in the required proportions and, to ensure homogeneity, blended in a planetary ball mill. The Retsch Planetary Ball Mill PM100 was used for blending with zirconia jars and 5 mm diameter zirconia balls at 300 rpm for 5 min. The blended powder was then pressed into pellets under a load of 3 tonnes (the load was adjusted to get pellets of uniform size without breaking). Multiple pellets of similar size were made for the different clinker raw meals[53]. The dimensions of the pellets were 16 mm in diameter and ~5 mm in height, weighing approximately 3 g each. The pellets were placed in an alumina crucible and heated in a Carbolite (RHF 14-35) muffle furnace with a maximum temperature of 1400 °C. The furnace was preheated, and the samples were placed in the furnace at 900 °C. The furnace was then heated to a target temperature varying between 1200 °C and 1310 °C at a rate of 5 °C min^{-1}, holding at that temperature for the corresponding dwell time as shown in Table 2. The samples are removed from the furnace after the dwell time and rapidly cooled with mechanically assisted air-cooling. The clinker samples were then stored in a vacuum desiccator for further characterization. The samples for SEM analysis were collected by breaking the clinker pellet into chunks, and the cross section of the pellet was used for the imaging, whereas the samples were ground into a fine powder (<63 µm) for XRD analysis, as discussed in Section 2.2.

The clinkering temperature was selected based on the stability and formation of ye'elimite in BCSA. Under normal pyroprocessing pressures, ye'elimite formation can start from 1000 °C and continue until 1300 °C, beyond which ye'elimite could decompose into other calcium aluminate phases[54]. The optimal temperature for clinkering for ye'elimite-rich cement was reported to be 1250 °C; however, this is also dependent on the raw materials used and the targeted clinker phase assemblage[17]. Thus, temperature ranges from 1200 °C to 1310 °C were selected.

Table 2. Clinkering condition: List of the different dwell temperatures and the corresponding dwelling times at the maximum temperature for the clinker samples.

Dwell temperature	Dwell time
1200 °C	1 h, 2 h
1220 °C	1 h, 2 h
1250 °C	1 h
1280 °C	15 min, 30 min, 45 min, and 1 h
1310 °C	1 h

2.4. Cement hydration

The ground clinker (<63 µm) was blended with 10 wt% gypsum to make the binder, which was mixed with distilled water at a water-binder ratio of 0.5 to make the cement paste samples. The cement paste samples were stored in sealed test tube vials at 20 °C for 56 d before testing. At 56 d, the samples were collected, and hydration was stopped based on the solvent exchange method using isopropyl alcohol (IPA). The samples were broken into smaller chunks (<5 mm) and immersed in IPA for 24 h, and then dried and stored in a vacuum desiccator until further material characterization was conducted; the sample was ground and characterized by XRD and TG (from STA).

3. Results and discussion

3.1. Raw materials characterization

The raw materials were characterized to determine the oxide composition for the raw mix design, as shown in Table 3. The two clay sources are termed Clay_1 and Clay_2, respectively. In addition to alumina and silica, Clay_1 had Mg and some alkalis as the main impurity, whereas Clay_2 had a significantly higher concentration of iron (Table 3). The difference in the loss of ignition (LOI) values between the clays can be mainly attributed to their different levels of moisture. The NMP sample has a negative LOI value as the sample would have some residual metal aluminium, and the oxidation (or even nitridation) of this would result in a mass gain.

3.2. Clinkering

BCSA clinker raw meals were formulated using the two sources of Clay_1 and Clay_2, designated as BCSA_1 and BCSA_2, respectively. The raw meals for the clinkers were designed based on stoichiometric calculations to achieve about 30% ye'elimite, 50%–60% belite, and 10% other phases (calcium sulfate and ferrite). The clinkers were made as per the clinkering conditions (Table 2) and analysed (Figs. 1 and 2). The quantification of the clinker phases showed that BCSA_1 did not have any residual calcium. Thus, additionally, BCSA_3 was formulated using Clay_1, designed to have a simi-

Table 3. Calculated oxide composition of the different raw materials as determined using XRF for elemental analyses.

Oxide composition	NMP	Gypsum	Clay_1	Clay_2
CaO	2.22	34.36	0.06	2.06
Al_2O_3	79.68	0.85	32.90	13.82
SiO_2	13.97	2.03	49.63	39.89
SO_3	0.66	51.09	0.00	3.38
Fe_2O_3	1.38	0.40	1.76	6.70
Na_2O	4.52	0.24	0.40	0.33
K_2O	0.85	0.22	5.43	2.48
Cl	0.36	0.00	0.00	0.00
MgO	4.13	0.00	2.85	0.42
P_2O_5	0.04	0.01	0.12	0.09
Mn_3O_4	0.28	0.02	0.32	0.32
TiO_2	0.76	0.00	0.39	0.72
LOI	(−) 8.9	10.8	6.14	29.8

lar amount of ye'elimite and belite but with an additional 10% calcium sulfate. BCSA_3 was specifically designed to monitor the desulfurization of calcium sulfate. A reference mix BCSA_4 was made using pure oxides of a similar target composition (30% ye'elimite, 60% belite) for comparison. Table 4 shows the raw meal proportions of the different raw materials and the oxide composition of the raw meal calculated based on the weight percentages in the raw meal and the respective oxide composition of the raw materials (from XRF). The clinkering was done as per the heating regime, as given in Table 2. The clinker samples were then ground and tested by XRD as mentioned in Section 2.2.

3.3. Clinker characterization

The X-ray diffractogram and quantification of the clinker phases of the BCSA clinkers synthesised at different temperatures and dwell times are shown in Figs. 1 and 2, respectively. In the BCSA_1 sample, most raw materials were consumed at 1200 °C, and free lime in the clinker was not detectable by XRD (Fig. 1). This indicates that most clinkering reactions were complete within 1 h at 1200 °C for the BCSA_1 sample. Furthermore, in the BCSA_1, with the increase in temperature, a steady but insignificant (within error) increase in the amount of ye'elimite formed was observed, without obvious differences in the overall clinker phase assemblage (Fig. 2). There were only trace amounts of gehlenite. The theoretically computed clinker phase also had a significant amount of ferrite and calcium sulfate phases, which were not observed in the clinker. This can be attributed to the iron being taken up by ye'elimite[55–57]. This is also reflected in the absence of calcium sulfate in the clinker, as it was consumed when aluminate and ferrites form ye'elimite. Only at higher temperatures (1280 °C and 1310 °C), the ferrite phase could be observed. Ye'elimite is known to decompose at higher temperatures over 1300 °C[54]; thus, the ferrite phase might start forming as the preferred phase only at elevated temperatures.

In BCSA_2, the clinkering conditions had a more significant impact on the clinker phases formed. At lower temperatures, there was a significant amount of free lime in the clinker, and it decreased when the dwell time increased to 2 h. For the BCSA_2 raw meal, a higher burning temperature or a longer dwell time was needed for the complete formation of the clinker phases. Only at 1280 °C, there was insignificant free lime left in the system (Fig. 2). BCSA_2 had a significantly higher amount of iron in the raw meal, which was reflected with a significant amount of ferrite phase formed in the clinker. Additionally, with the increase in temperature or dwell time, the amount of ye'elimite formed reduced. Although the clinkering process was not completed, the ye'elimite amount reduction indicates its decomposition (loss of sulfate as SO_2 and O_2)[15]. This can be attributed to iron content, which can promote the decomposition of ye'elimite (at a lower temperature) and increase the rate of desulfurization from calcium sulfate[55,58]. On the other hand, iron has also been reported to facilitate the formation of ye'elimite at a lower temperature[55,59], unlike the observations from

Table 4. Raw meal composition with the theoretical oxide composition and the predicted clinker phase calculated based on stoichiometry for the different clinker (wt%).

Raw material	BCSA_1	BCSA_2	BCSA_3	BCSA_4
Limestone	59.89	60.23	58.38	
Clay_1	24.21		23.31	
Clay_2		21.09		
Gypsum	10.37	5.82	14.45	
NMP	5.53	12.36	3.85	
RG-$CaCO_3$				61.38
RG-Al_2O_3				10.96
RG-$CaSO_4$				12.41
RG-SiO_2				15.25
Theoretical oxide composition	BCSA_1	BCSA_2	BCSA_3	BCSA_4
CaO	37.35	36.67	37.98	39.50
Al_2O_3	12.65	13.10	11.51	10.96
SiO_2	13.82	13.44	13.73	15.25
Fe_2O_3	0.83	2.16	0.57	0.00
SO_3	5.50	4.14	7.72	7.30
CO_2	26.33	26.48	25.67	26.99
Others	2.74	2.99	2.83	-
Theoretical clinker phase composition	BCSA_1	BCSA_2	BCSA_3	BCSA_4
Ye'elimite	34.25	32.08	29.91	29.90
Belite	55.84	53.45	52.94	59.80
Anhydrite	5.19	2.54	10.99	10.30
Ferrite	2.43	9.10	2.32	0
Rest	2.29	2.83	3.84	-

Note: RG = reagent grade.

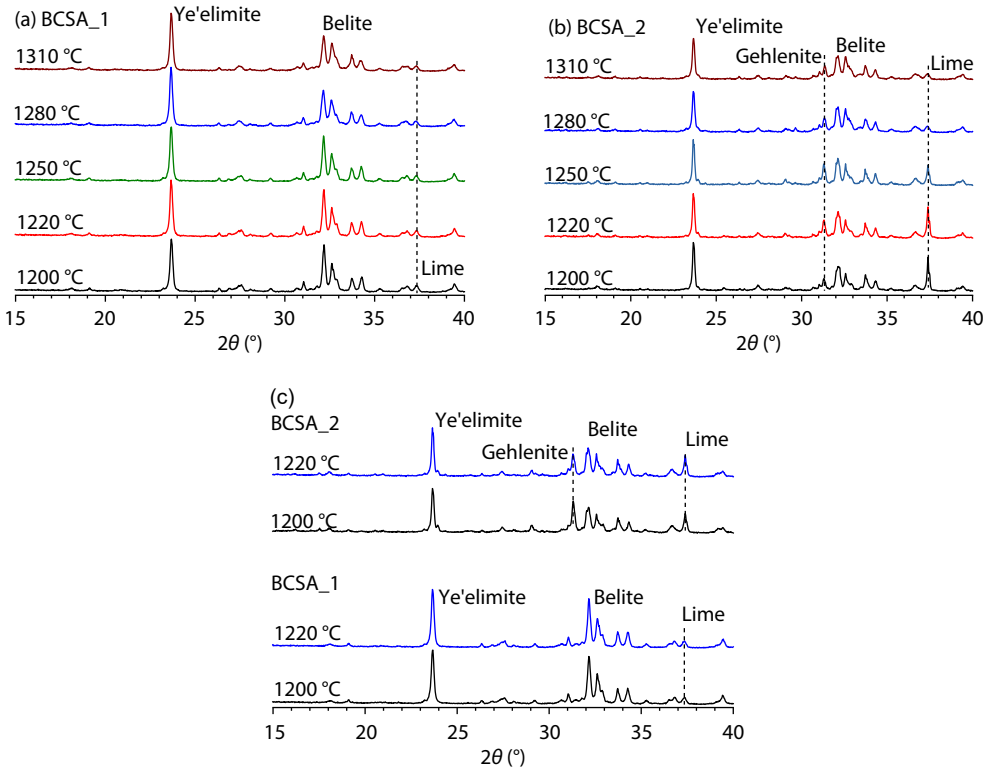

Fig. 1. X-ray diffractograms of clinker synthesised at different temperatures and dwell times: (a) BCSA_1 with a dwell time of 1 h, (b) BCSA_2 with a dwell time of 1 h, and (c) BCSA_1 and BCSA_2 with a dwell time of 2 h. Note: Dashed lines represent the main peaks of gehlenite and lime for reference.

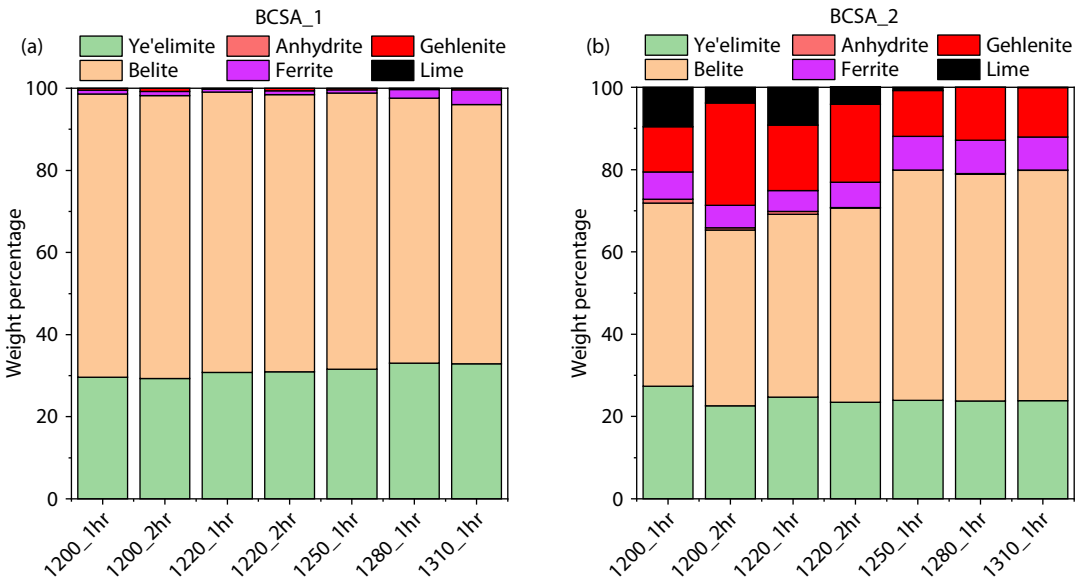

Fig. 2. Clinker phase composition for (a) BCSA_1 and (b) BCSA_2 synthesised at different temperatures and dwell times computed by quantitative X-ray diffraction (QXRD).

BCSA_2. The stability of ye'elimite at lower temperatures could have been affected by the other minor elements like phosphorus or magnesium (from Clay_2) on the clinkering reaction[60]; however, further studies are needed to understand their role and effect. BCSA_2 also showed the formation of gehlenite phase in the clinker, which can be attributed to the loss of sulfate, perhaps assisted by the presence of iron. The preferred formation of gehlenite over belite could also be attributed to its lower Gibbs free energy[61].

The raw meal of BCSA_1 made using NMP and Clay_1 was easier to produce and required less energy. Furthermore, shorter dwell times at 1280 °C were attempted using the raw meal prepared from NMP and Clay_1 (BCSA_3). As the BCSA_1 clinker did not have any calcium sulfate, the amount of calcium sulfate for the targeted composition increased by 5% (Table 4). This raw meal formed ye'elimite and belite at

1280 °C with a dwell time of as little as 15 min, and there was no detectable amount of free lime in the clinker (Fig. 3). This indicates that the clinkering reaction required only 15 min (or less) for the formation of ye'elimite and belite. Similar observations have been made of lower dwell time required for the formation of ye'elimite at higher temperatures (1300 °C)[54,59]. The phase composition of ye'elimite and belite did not significantly change from 15 min to 1 h; however, the detectable amount of calcium sulfate seemed to reduce from about 2.5% to an undetectable level at 1 h (which is probably within the error). At 1280 °C, calcium sulfate seems to be stable when it forms ye'elimite; the excess calcium sulfate (in the raw meal) reduces rapidly and is lost due to desulfurization after 15 min. The presence of iron in the raw meal could have also enhanced the desulfurization of calcium sulfate[55,58]. In addition to the calcium sulfate being consumed to form additional ye'elimite (incorporating iron), some of the calcium sulfate is also lost during the clinkering process.

3.4. Clinkering reactions

The two BCSA_1 and BCSA_2 clinker made using the different sources of clays were compared against BCSA_4 with similar composition but made using pure reagent-grade simple oxide phases. The DSC data indicate regions of phase changes/chemical reactions taking place (Fig. 4). The strong endothermic peak near 800 °C is attributed to the decarbonation of $CaCO_3$[54,62]. The heat flow corresponding to the decarbonation of $CaCO_3$ in the BCSA_1 sample is very similar to that in the BCSA_4 sample, whereas there is a slight shift in the peak for the BCSA_2 sample. This change may be attributed to the fact that BCSA_2 has a higher iron content and other minor elements[60,63,64]. The BCSA_4 sample had a minor exothermic peak near 900 °C, which may be attributed to the crystallization of some raw material or clinker phases[54]; however, this peak is absent for the clinkers with waste clay. Beyond 900 °C, all the samples had a continuous heat release, indicating the clinkering reaction taking place. The formation of belite from lime and silica is an exothermic reaction[65]. The peak for belite formation appears before 1200 °C for the samples using waste clay, whereas for BCSA_4, the peak appears later, beyond 1200 °C[63]. The presence of iron and other minor elements (from the raw meal) could enhance the reaction of belite formation. Additionally, the source of silica for the BCSA_4 raw meal was crystalline silica (reagent grade), which would have lower reactivity than the silica available from the clay sources. The clinker reactions for ye'elimite started beyond 1200 °C. In the pure phase BCSA_4 clinker, two sharp endothermic peaks were observed at 1220 °C and 1260 °C, corresponding to the transition of calcium sulfate phase and the formation of ye'elimite, respectively[59,60]. Beyond 1300 °C, there was a broad endothermic peak accompanied by mass loss in the sample, which can be attributed to the decomposition of ye'elimite and calcium sulfate[54,58]. Whereas in BCSA_1 and BCSA_2, there was a single broader exothermic region at 1200 °C. The zone could indicate the overlapping peaks of the transition of calcium sulfate, the formation of ye'elimite, and the decomposition of calcium sulfate[54,62]. These changes from the BCSA_4 sample could be attributed to the presence of iron and other minor elements from the raw meal; further studies and detailed characterization are required to understand this. For further SEM characterization and hydration studies, one of the samples (BCSA_1 synthesised at 1280 °C with a dwell time of 1 h) was chosen.

3.5. Phase and elemental maps of the BCSA_1 clinker

BCSA_1 clinker sample (made at 1280 °C with a dwell time of 1 h) was selected for further characterization and phase mapping using SEM-EDS analysis. The elemental composition data from the EDS map were collected and used to make the phase maps. The SEM-BSE image distinctly shows two different phases, with a brighter and darker phase visible, with some void spaces (Fig. 5a). The clinker sample, unlike PC, did not have a continuously filled solid structure; the clinker was formed with voids or pores. BCSA cements have been

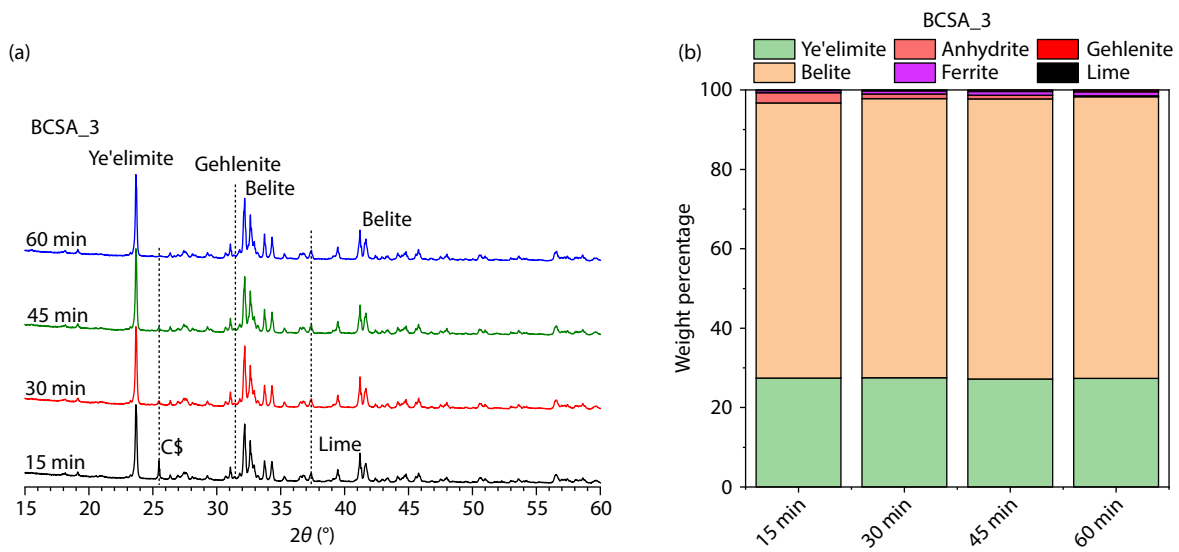

Fig. 3. (a) X-Ray diffractograms and (b) the quantified phase composition of BCSA_3 clinker synthesised at 1280 °C with a dwell time of 15 min to 60 min. Note: Dashed lines represent the main peaks of gehlenite and lime for reference.

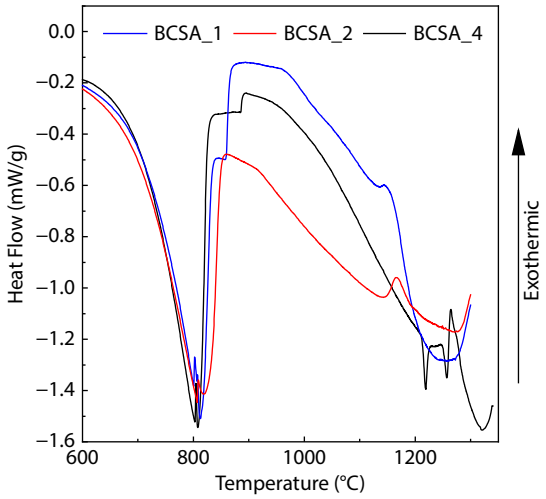

Fig. 4. Heat flow curves from DSC analysis (phases under an air atmosphere heated at 10 °C min^{-1}) comparing the different batches of BCSA raw meal made using industrial by-products (BCSA_1 and BCSA_2) and reagent-grade oxides (BCSA_4).

reported to form a more porous clinker[18]. The SEM-EDS analysis of the individual elements and phase map of the clinker phases is shown in Fig. 5b and Fig. 5c, respectively. The brighter phases were found to be belite, and the darker phases were ye'elimite based on the phase mapping (Fig. 5c). The clinker phases predominantly contained calcium, silicon, aluminium, and sulphur as the main elements with minor amounts of magnesium and iron, as expected from the raw meal. The distribution of calcium was more concentrated in the belite region than in ye'elimite (ye'elimite, based on stoichiometry, has a lesser demand for calcium). The presence of silicon and aluminium was limited to the region of belite and ye'elimite, respectively. Calcium sulfate deposits were found within the belite crystal, and magnesium was found in ye'elimite. Although the magnesium was concentrated in a small region, it also showed signals from calcium, aluminium, and sulphur, which could indicate a small deposit of MgO or intermixing and incorporation of magnesium in ye'elimite. However, further detailed investigation is required to confirm this. Similarly, although the concentration of iron was low, its distribution was also observed only in the ye'elimite region. This indicates the incorporation of iron within the ye'elimite structure and not forming a separate clinker phase. No other deleterious elements and minor elements (from the raw meal) were detected in the clinker phases.

3.6. Hydration reactions of BCSA_1

Hydration studies were conducted using the BCSA_1 (synthesised at 1280 °C with a dwell time of 1 h) clinker blended with 10% gypsum. Cement paste samples were prepared at a water-binder ratio of 0.5 and cured under sealed conditions at 20 °C for 56 d. A longer duration of curing (56 d rather than 28 d) was selected for the preliminary study to allow sufficient time for belite hydration. The hydrated cement paste sample was characterized using XRD and TG (from STA). The ye'elimite phase in the clinker was completely consumed during this period, with belite also starting to hydrate (Fig. 6). The diffractogram clearly shows the main hydration products

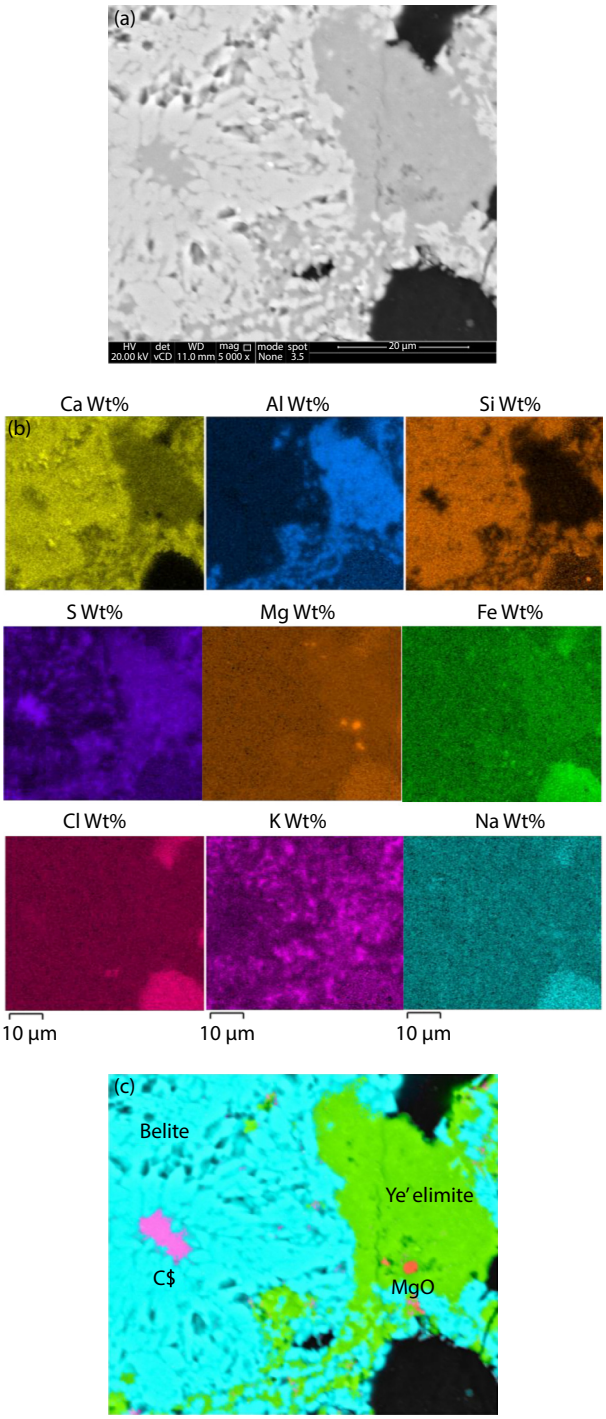

Fig. 5. (a) SEM-BSE image of BCSA_1 clinker captured on the cross-section of a clinker polished section showing the different clinker phases. (b) The elemental distribution map represented using data of the individual elements from SEM-EDS analysis done on a cross-section of BCSA_1 clinker in a polished section. (c) Phase mapping of the different clinker phases made using data of elemental distribution from SEM-EDS analysis done on a cross-section of BCSA_1 clinker in a polished section. Note: The different phases have been highlighted using different colours—blue: belite, green: ye'elimite, pink: calcium sulfate (C$), and red: MgO and ye'elimite.

of ettringite and strätlingite from the hydration of ye'elimite and belite, respectively, whereas the aluminium hydroxide formed (generally amorphous or microcrystalline) was better

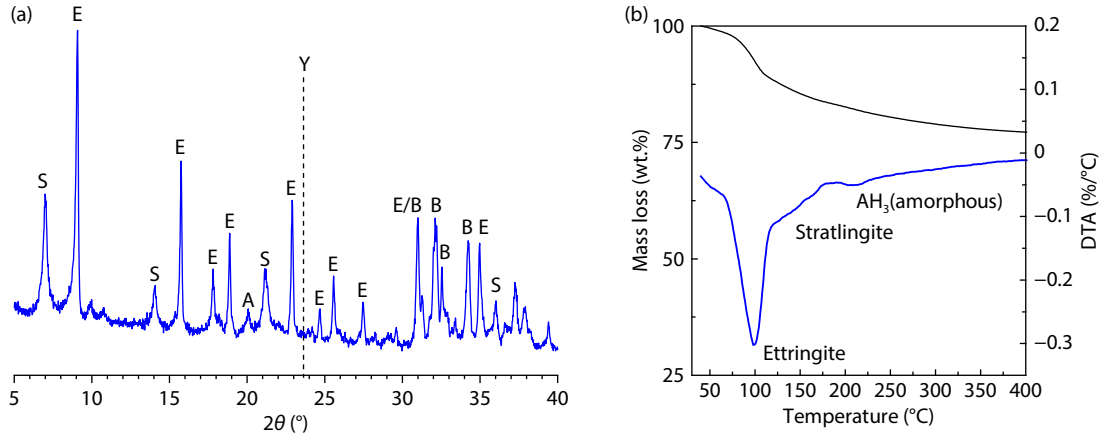

Fig. 6. (a) X-ray diffractogram and (b) mass loss from thermogravimetric analysis data of hydrated BCSA_1 cement (synthesised at 1280 °C with a dwell time of 1 h) blended with 10% gypsum at a 0.5 water-binder ratio at 56 d. Note: S: Strätlingite, E: Ettringite, B: Belite, A: Aluminium hydroxide[66], and the main peak of ye'elimite (Y) marked with a dashed line.

detected in thermogravimetric analysis[36,66,67]. The TG data also support/supplement the XRD data, showing a clear peak defined for ettringite and mass loss observed in regions corresponding to strätlingite and aluminium hydroxide. With sufficient gypsum, ye'elimite completely reacted to form ettringite and aluminium hydroxide, and the belite formed strätlingite. The formation of strätlingite confirms the reactivity of belite and indicates that belite will continue to hydrate to fill the pores and improve durability[35,36,67].

4. Conclusions and closing remarks

(1) The non-metallic by-product from the secondary aluminium treatment industry was used to meet the alumina requirements for BCSA clinker. BCSA clinker of the targeted composition was successfully synthesised using the locally available waste clays and NMP from the UK.

(2) The produced clinker did not show any detectable presence of deleterious elements as observed by XRD and SEM-EDS.

(3) Results indicate that it is easier to form BCSA with diminished iron oxide content and/or from kaolinite-rich clays poor in iron, even with only 15 min in the clinkering zone.

(4) Iron and minor elements in the raw meal influenced the clinker-forming process, as observed in the changes in heat flow during the formation of clinker phases.

(5) The BCSA made with Clay_1 was hydrated with gypsum and was shown to have sufficient reactivity with the complete consumption of ye'elimite and initial reaction of belite.

(6) The primary hydration products of the BCSA cement were ettringite, strätlingite, and aluminium hydroxide.

Author contribution statement

Vaishnav Kumar Shenbagam: Conceptualization, Data curation, Formal analysis, Investigation, Methodology, Project administration, Writing – original draft, Writing – review & editing. **Rand Hadi Farhan:** Investigation, Writing – original draft, Writing – review & editing. **Theodore Hanein:** Conceptualization, Formal analysis, Funding acquisition, Investigation, Methodology, Project administration, Writing – original draft, Writing – review & editing.

Declaration of competing interest

Theodore Hanein is an Associate Editor for *Materials Reports: Solidwaste and Ecomaterials* and was not involved in the editorial review or the decision to publish this article. The authors declare the following financial interests/personal relationships which may be considered as potential competing interests: Rand Hadi Farhan is employed by Altek Europe.

Acknowledgements

The work was funded by UKRI through Future Leaders Fellowship (MR/V023829/1): "Green, Circular, and Smart Cement Manufacture". The authors would like to thank all the advisory board members for their insights and guidance. We specifically thank Altek (Harsco), Imerys, British Gypsum (Saint Gobain), and ARUP for providing us with the raw [waste] materials for the study.

References

[1] Information on https://www.iea.org/data-and-statistics/charts/global-cement-production-in-the-net-zero-scenario-2010-2030-5260 (cited 26 August 2024).

[2] Gálvez-Martos, J. L., Valente, A., Martínez-Fernández, M., et al. Eco-efficiency assessment of calcium sulfoaluminate clinker production. *Journal of Industrial Ecology*, **2020**, 24(3): 695–706. https://doi.org/10.1111/jiec.12967.

[3] Terán-Cuadrado, G., Tahir, F., Nurdiawati, A., et al. Current and potential materials for the low-carbon cement production: Life cycle assessment perspective. *Journal of Building Engineering*, **2024**, 96: 110528. https://doi.org/10.1016/j.jobe.2024.110528.

[4] Gartner, E., Sui, T. Alternative cement clinkers. *Cement and Concrete Research*, **2018**, 114: 27–39. https://doi.org/10.1016/j.cemconres.2017.02.002.

[5] Hanein, T., Torre, A.G. De la, Zhang, Z., Provis, J.L. Alternative Non-Portland Binders. *Elements*, **2022**, 18(5): 314–320. https://doi.org/10.2138/gselements.18.5.314.

[6] Hanein, T., Galvez-Martos, J. L., Bannerman, M. N. Carbon footprint of calcium sulfoaluminate clinker production. *Journal of Cleaner Production*, **2018**, 172: 2278–2287. https://doi.org/10.1016/j.jclepro.2017.11.183.

[7] Gartner, E. Industrially interesting approaches to "low-CO_2" cements. *Cement and Concrete Research*, **2004**, 34(9): 1489–1498. https://doi.org/10.1016/j.cemconres.2004.01.021.
[8] Bescher, E., Kim, J. Belitic Calcium Sulfoaluminate Cement: History, Chemistry, Performance, and Use in the United States, Conference: 1st International Conference on Innovation in Low Carbon Cement and Concrete Technology, **2019**: 2–5.
[9] K. Alexander, Expansive and shrinkage-compensated cements, US3251701A, 1966. https://patents.google.com/patent/US3251701A/en (cited 14 October 2024).
[10] Alexander, K. Studies of calcium sulpho aluminate admixtures for expansive cements. In: Proceedings of ASTM 58, **1958**: 968–1008.
[11] Zhang, L., Su, M., Wang, Y. Development of the use of sulfo- and ferroaluminate cements in China. *Advances in Cement Research*, **1999**, 11(1): 15–21. https://doi.org/10.1680/adcr.1999.11.1.15.
[12] Hanein, T., Gálvez-Martos, J.L., Bescher, E. The Role of Belitic Calcium Sulfoaluminate Cement in Achieving Net-zero. In: 16th International Congress on the Chemistry of Cement, Further Reduction of CO2 -Emissions and Circularity in the Cement and Concrete Industry, Bangkok, **2023**.
[13] Bescher, E. Belitic calcium sulfoaluminate cement: Hydration chemistry, performance, and use in the United States. In: 15th International Congress on the Chemistry of Cement, Prague, **2019**.
[14] Sharp, J. H., Lawrence, C. D. , Yang, R. *Calcium sulfoaluminate cements: Low-energy cements, special cements or what?Advances in Cement Research*, **1999**, 11(1): 3–13. https://doi.org/10.1680/adcr.1999.11.1.3.
[15] Hanein, T., Galan, I., Elhoweris, A., et al. Production of belite calcium sulfoaluminate cement using sulfur as a fuel and as a source of clinker sulfur trioxide: Pilot kiln trial. *Advances in Cement Research*, **2016**, 28(10): 643–653. https://doi.org/10.1680/jadcr.16.00018.
[16] Lothenbach, B., Geiger, C. A., Dachs, E., et al. Thermodynamic properties and hydration behavior of ye'elimite. *Cement and Concrete Research*, **2022**, 162: 106995. https://doi.org/10.1016/j.cemconres.2022.106995.
[17] Ben Haha, M., Winnefeld, F., Pisch, A. Advances in understanding ye'elimite-rich cements. *Cement and Concrete Research*, **2019**, 123: 105778. https://doi.org/10.1016/j.cemconres.2019.105778.
[18] Zhang, L. Microstructure and performance of calcium sulfoaluminate cements. Ph.D. Dissertation. Aberdeen, Scotland, UK: University of Aberdeen, **2000**.
[19] Isteri, V., Ohenoja, K., Hanein, T., et al. Ferritic calcium sulfoaluminate belite cement from metallurgical industry residues and phosphogypsum: Clinker production, scale-up, and microstructural characterisation. *Cement and Concrete Research*, **2022**, 154: 106715. https://doi.org/10.1016/j.cemconres.2022.106715.
[20] Arjunan, P., Silsbee, M. R., Della M Roy. Sulfoaluminate-belite cement from low-calcium fly ash and sulfur-rich and other industrial by-products. *Cement and Concrete Research*, **1999**, 29(8): 1305–1311. https://doi.org/10.1016/S0008-8846(99)00072-1.
[21] Canbek, O., Shakouri, S., Erdoğan, S. T. Laboratory production of calcium sulfoaluminate cements with high industrial waste content. *Cement and Concrete Composites*, **2020**, 106: 103475. https://doi.org/10.1016/j.cemconcomp.2019.103475.
[22] Isteri, V., Ohenoja, K., Hanein, T., et al. Production and properties of ferrite-rich CSAB cement from metallurgical industry residues. *Science of The Total Environment*, **2020**, 712: 136208. https://doi.org/10.1016/j.scitotenv.2019.136208.
[23] Isteri, V., Ohenoja, K., Rößler, C., et al. The effect of slag variability in the attempted manufacture of AYF (alite-ye'elimite-ferrite) cement clinker at both laboratory and pilot scale. *CEMENT*, **2024**, 16: 100098. https://doi.org/10.1016/j.cement.2024.100098.
[24] Majling, J., Sahu, S., Vlna, M., et al. Relationship between raw mixture and mineralogical composition of sulphoaluminate belite clinkers in the system CaO–SiO_2–Al_2O_3–Fe_2O_3–SO_3. *Cement and Concrete Research*, **1993**, 23(6): 1351–1356. https://doi.org/10.1016/0008-8846(93)90072-H.
[25] Marroccoli, M., Telesca, A., Lothenbach, B., et al. Synthesis and properties of a belite–calcium sulfoaluminate cement obtained using only waste materials. *Advances in Cement Research*, **2025**, 37(2): 78–88. https://doi.org/10.1680/jadcr.24.00005.
[26] Ren, C., Wang, W., Li, G. Preparation of high-performance cementitious materials from industrial solid waste. *Construction and Building Materials*, **2017**, 152: 39–47. https://doi.org/10.1016/j.conbuildmat.2017.06.124.
[27] Telesca, A., Marroccoli, M., Tomasulo, M., et al. Low-CO_2Cements from fluidized bed process wastes and other industrial by-products. *Combustion Science and Technology*, **2016**, 188(4/5): 492–503. https://doi.org/10.1080/00102202.2016.1138736.
[28] Telesca, A., Matschei, T., Marroccoli, M. Study of eco-friendly belite-calcium sulfoaluminate cements obtained from special wastes. *Applied Sciences*, **2020**, 10(23): 8650. https://doi.org/10.3390/app10238650.
[29] Lyu, H., Zhang, S., Poon, C. S. Synthesis of hydraulic waste-derived belite-rich calcium sulfoaluminate clinker: Feedstock design, component calculation, and clinkering optimization. *Cement and Concrete Composites*, **2024**, 153: 105714. https://doi.org/10.1016/j.cemconcomp.2024.105714.
[30] Fan, C., Wang, B., Xu, Y. Solidification/stabilization and immobilization mechanism of Pb(II) and Zn(II) in ettringite. *Cement and Concrete Research*, **2023**, 174: 107350. https://doi.org/10.1016/j.cemconres.2023.107350.
[31] Kearney, S., Yorkshire, A. S., Geddes, D. A., et al. Chapter 25 Cement-based stabilization/solidification of radioactive waste. *Low Carbon Stabilization and Solidification of Hazardous Wastes*, **2022**: 407–431. https://doi.org/10.1016/B978-0-12-824004-5.00005-0.
[32] Gougar, M. L. D., Scheetz, B. E., Roy, D. M. Ettringite and C–S–H Portland cement phases for waste ion immobilization: A review. *Waste Management*, **1996**, 16(4): 295–303. https://doi.org/10.1016/S0956-053X(96)00072-4.
[33] Cholostiakow, S., Ren, Z., Skyrianou, I., et al. Bond of textile-reinforced belite calcium sulfoaluminate cement mortar to concrete substrate. *Materials and Structures*, **2024**, 57(4): 82. https://doi.org/10.1617/s11527-024-02347-5.
[34] Shenbagam, V. K., Chaunsali, P. Influence of calcium hydroxide and calcium sulfate on early-age properties of non-expansive calcium sulfoaluminate belite cement. *Cement and Concrete Composites*, **2022**, 128: 104444. https://doi.org/10.1016/j.cemconcomp.2022.104444.
[35] Winnefeld, F., Lothenbach, B. Hydration of calcium sulfoaluminate cements: Experimental findings and thermodynamic modelling. *Cement and Concrete Research*, **2010**, 40(8): 1239–1247. https://doi.org/10.1016/j.cemconres.2009.08.014.
[36] Mrak, M., Winnefeld, F., Lothenbach, B., et al. The influence of calcium sulfate content on the hydration of belite-calcium sulfoaluminate cements with different clinker phase compositions. *Materials and Structures*, **2021**, 54(6): 212. https://doi.org/10.1617/s11527-021-01811-w.
[37] Aranda, M.A.G., Torre, A.G. De la. Sulfoaluminate cement. *Eco-Efficient Concrete*, **2013**: 488–522. https://doi.org/10.1533/9780857098993.4.488.
[38] Ambrose, J., Shenbagam, V. K., Provis, J. L., et al. Assessment of standard test procedures applied to calcium sulfoaluminate based cements. *Advances in Cement Research*, **2025**, 37(2):

125–132. https://doi.org/10.1680/jadcr.24.00033.
[39] Gálvez-Martos, J. L., Chaliulina, R., Elhoweris, A., et al. Techno-economic assessment of calcium sulfoaluminate clinker production using elemental sulfur as raw material. *Journal of Cleaner Production*, **2021**, 301: 126888. https://doi.org/10.1016/j.jclepro.2021.126888.
[40] Tsakiridis, P. E. Aluminium salt slag characterization and utilization–A review. *Journal of Hazardous Materials*, **2012**, 217: 1–10. https://doi.org/10.1016/j.jhazmat.2012.03.052.
[41] Gil, A., Korili, S. A. Management and valorization of aluminum saline slags: Current status and future trends. *Chemical Engineering Journal*, **2016**, 289: 74–84. https://doi.org/10.1016/j.cej.2015.12.069.
[42] Bide, T., Brown, T.J., Idoine, N.E., Mankelow, J. United Kingdom Minerals Yearbook 2020. **2021**.
[43] Piperopoulos, K., Kaldellis, A., Oustadakis, P., et al. Valorization of aluminum salt slag washed residue in the production of Portland cement clinker. *Journal of Sustainable Metallurgy*, **2022**, 8(1): 102–111. https://doi.org/10.1007/s40831-022-00504-0.
[44] Satish Reddy, M., Neeraja, D. Aluminum residue waste for possible utilisation as a material: A review. *Sādhanā*, **2018**, 43(8): 124. https://doi.org/10.1007/s12046-018-0866-2.
[45] Tsakiridis, P. E., Oustadakis, P., Agatzini-Leonardou, S. Black dross leached residue: An alternative raw material for Portland cement clinker. *Waste and Biomass Valorization*, **2014**, 5(6): 973–983. https://doi.org/10.1007/s12649-014-9313-8.
[46] Cuesta, A., De La Torre, A.G., Losilla, E.R., Peterson, V.K., Rejmak, P., Ayuela, A., et al. Structure, Atomistic Simulations, and Phase Transition of Stoichiometric Yeelimite. *Chemistry of Materials*, **2013**, 25: 1680–1687. https://doi.org/10.1021/cm400129z.
[47] Mumme, W., Hill, R. J., Bushnell-wye, G., et al. Rietveld crystal structure refinements, crystal chemistry and calculated powder diffraction data for the polymorphs of dicalcium silicate and related phases.
[48] Kirfel, A., Will, G. Charge density in anhydrite, $CaSO_4$, from X-ray and neutron diffraction measurements. *Acta Crystallographica Section B*, **1980**, 36(12): 2881–2890. https://doi.org/10.1107/S0567740880010461.
[49] Redhammer, G. J., Tippelt, G., Roth, G., et al. Structural variations in the brownmillerite series $Ca_2(Fe_{2-x}Al_x)O_5$: Single-crystal X-ray diffraction at 25 °C and high-temperature X-ray powder diffraction (25 °C ⩽*T*⩽ 1000 °C).*American Mineralogist*, **2004**, 89(2/3): 405–420. https://doi.org/10.2138/am-2004-2-322.
[50] Mondal, P., Jeffery, J. W. The crystal structure of tricalcium aluminate, $Ca_3Al_2O_6$. *Acta Crystallographica Section B Structural Crystallography and Crystal Chemistry*, **1975**, 31(3): 689–697. https://doi.org/10.1107/s0567740875003639.
[51] Louisnathan, S.J. Refinement of the crystal structure of a natural gehlenite, Ca_2 $Al(Al,Si)_2O_7$. *The Canadian Mineralogist*, **1971**, 10(5): 822–837.
[52] Irran, E., Tillmanns, E., Hentschel, G. Ternesite, $Ca_5(SiO4)_2SO4$, a new mineral from the ettringer bellerberg/Eifel, Germany. *Mineralogy and Petrology*, **1997**, 60(1): 121–132. https://doi.org/10.1007/BF01163138.
[53] Simoni, M., Hanein, T., Duvallet, T. Y., et al. Producing cement clinker assemblages in the system: $CaO\text{-}SiO_2\text{-}Al_2O_3\text{-}SO_3\text{-}CaCl_2$-MgO. *Cement and Concrete Research*, **2021**, 144: 106418. https://doi.org/10.1016/j.cemconres.2021.106418.
[54] El Khessaimi, Y., El Hafiane, Y., Smith, A., et al. Solid-state synthesis of pure ye'elimite. *Journal of the European Ceramic Society*, **2018**, 38(9): 3401–3411. https://doi.org/10.1016/j.jeurceramsoc.2018.03.018.
[55] Bullerjahn, F., Scholten, T., Scrivener, K. L., et al. Formation, composition and stability of ye'elimite and iron-bearing solid solutions. *Cement and Concrete Research*, **2020**, 131: 106009. https://doi.org/10.1016/j.cemconres.2020.106009.
[56] Chen, D., Feng, X., Long, S. The influence of ferric oxide on the properties of $3CaO \cdot 3Al_2O_3 \cdot CaSO_4$. *Thermochimica Acta*, **1993**, 215: 157–169. https://doi.org/10.1016/0040-6031(93)80089-S.
[57] Thaivalappil, B., Chaunsali, P. Influence of iron content on processing conditions and early age hydration of ye'elimite. *Materials Today: Proceedings*, **2023**. https://doi.org/10.1016/j.matpr.2023.07.004.
[58] Yan, Z., Wang, Z., Liu, H., et al. Decomposition and solid reactions of calcium sulfate doped with SiO_2, Fe_2O_3 and Al_2O_3. *Journal of Analytical and Applied Pyrolysis*, **2015**, 113: 491–498. https://doi.org/10.1016/j.jaap.2015.03.019.
[59] Zhang, Y., Li, X., Shen, X. Kinetics of calcium sulfoaluminate with 1% iron oxide by isothermal and isoconversional methods. *Advances in Cement Research*, **2017**, 29(8): 336–346. https://doi.org/10.1680/jadcr.16.00150.
[60] Benarchid, M. Y., Rogez, J. The effect of Cr_2O_3 and P_2O_5 additions on the phase transformations during the formation of calcium sulfoaluminate C4A3 S^-. *Cement and Concrete Research*, **2005**, 35(11): 2074–2080. https://doi.org/10.1016/j.cemconres.2005.06.005.
[61] Pimraksa, K., Hanjitsuwan, S., Chindaprasirt, P. Synthesis of belite cement from lignite fly ash. *Ceramics International*, **2009**, 35(6): 2415–2425. https://doi.org/10.1016/j.ceramint.2009.02.006.
[62] Huang, Y., Pei, Y., Qian, J., et al. Bauxite free iron rich calcium sulfoaluminate cement: Preparation, hydration and properties. *Construction and Building Materials*, **2020**, 249: 118774. https://doi.org/10.1016/j.conbuildmat.2020.118774.
[63] Luo, L., Zhang, Y., Bao, S., et al. Utilization of iron ore tailings as raw material for Portland cement clinker production. *Advances in Materials Science and Engineering*, **2016**, 2016(1): 1596047. https://doi.org/10.1155/2016/1596047.
[64] Wang, X., Sun, K., Li, X., et al. The effect of red mud on sintering processes and minerals of Portland cement for roads. *Crystals*, **2021**, 11(10): 1267. https://doi.org/10.3390/cryst11101267.
[65] Taylor, H.F.W. Cement chemistry, 2nd edition. London: Thomas Telford Ltd.**1997**.
[66] Winnefeld, F., Barlag, S. Calorimetric and thermogravimetric study on the influence of calcium sulfate on the hydration of ye'elimite. *Journal of Thermal Analysis and Calorimetry*, **2010**, 101(3): 949–957. https://doi.org/10.1007/s10973-009-0582-6.
[67] Álvarez-Pinazo, G., Santacruz, I., Aranda, M. A. G., et al. Hydration of belite–ye'elimite–ferrite cements with different calcium sulfate sources. *Advances in Cement Research*, **2016**, 28(8): 529–543. https://doi.org/10.1680/jadcr.16.00030.

Vaishnav Kumar Shenbagam is currently a postdoctoral research fellow in the School of Civil Engineering at the University of Leeds. He holds B.Tech and M. Tech degrees in civil engineering from the National Institute of Technology, Tiruchirappalli, and the Indian Institute of Technology, Madras, respectively. He completed his PhD from the Indian Institute of Technology, Madras, working on calcium sulfoaluminate-based binders. His research interests include cement chemistry, hydration characteristics of cement, and mechanical and durability studies in cement concrete. His current research focuses on synthesizing and developing alternative low-CO_2 binder systems, such as the calcium sulfoaluminate-based binders.

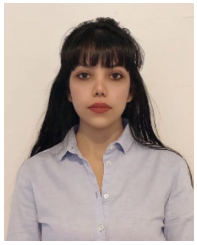

Rand Hadi Farhan is a doctoral researcher in the Materials Science and Engineering Department at the University of Sheffield and is working with Professor Theodore Hanein on the Future Leadership Fellowship Project (Green, Circular, and Smart Cement Manufacture). Currently, she is on a placement at Altek Europe Limited Company, taking a role as a materials scientist and engineer in the ALUSALT project at the Engineering and Technology Department. Following her bachelor's degree in geology, she graduated in 2022 from the University of Edinburgh with a master's degree in geoenergy with research focuses on carbon capture and storage, carbon mineralization, renewable energy, and energy transition. Her current research focuses on the manufacturing of low-carbon cement (calcium sulfoaluminate (CSA) cement) by valorising industrial by-products.

Theodore Hanein is a UKRI Future Leaders Fellow on Green, Circular, and Smart Cement Manufacture. Following his two undergraduate degrees in Chemistry and Chemical Engineering, he graduated from the University of Manchester (2012) with a Master's in Advanced Process Design and Integration, and then from the University of Aberdeen (2016) with a PhD in Cement/Clinker Thermochemistry. Following graduation, he began working at the University of Sheffield on low-carbon cement and concrete, where he was promoted twice from postdoctoral researcher to assistant professor and then associate professor, before joining the University of Leeds. His work centres around sustainable materials and processes.